On restraining the production of small scales of motion in a turbulent channel flow

Verstappen, Roel

Published in:
Computers & fluids

DOI:
10.1016/j.compfluid.2007.01.013

Publication date:
2008

Available online at www.sciencedirect.com
ScienceDirect
Computers & Fluids 37 (2008) 887–897
computers & fluids
www.elsevier.com/locate/compfluid

On restraining the production of small scales of motion in a turbulent channel flow

Roel Verstappen *

Institute of Mathematics and Computing Science, University of Groningen, P.O. Box 800, 9700 AV Groningen, The Netherlands

Received 1 October 2006; received in revised form 18 December 2006; accepted 16 January 2007
Available online 29 September 2007

Abstract

Since most turbulent flows cannot be computed directly from the incompressible Navier–Stokes equations, a dynamically less complex mathematical formulation is sought. In the quest for such a formulation, we consider nonlinear approximations of the convective term that preserve the symmetry and conservation properties. In particularly, the energy, enstrophy (in 2D) and helicity are conserved. The underlying idea is to restrain the convective production of small scales in an unconditional stable manner, meaning that the approximate solution cannot blow up in the energy-norm (in 2D also: enstrophy-norm). The numerical algorithm used to solve the governing equations preserves the symmetry and conservation properties too. The resulting simulation method is successfully tested for a turbulent channel flow ($Re_\tau = 180$ and 395).

1. Introduction

The Navier–Stokes equations provide an appropriate model for turbulent flow. In the absence of compressibility ($\nabla \cdot u = 0$), the equations are

$$\partial_t u + \mathscr{C}(u,u) + \mathscr{D}(u) + \nabla p = 0, \tag{1}$$

where u denotes the instantaneous fluid velocity field, and p stands for the pressure. The linear term $\mathscr{D}(u) = -\Delta u/Re$ (Re is the Reynolds number) is dissipative. It is the most effective at the smallest scales of motion. The nonlinear term $\mathscr{C}(u,v) = (u \cdot \nabla)v$ transfers energy from the scales at which the flow is driven to the smallest ones that survive dissipation. Attempts at simulating turbulence directly from the Navier–Stokes equations are limited to "a millisecond over a postage stamp" [1], because the nonlinear term produces simply too many scales of motion. Therefore a dynamically less complex mathematical formulation is sought.

In the quest for such a formulation, the Navier–Stokes equations may be filtered spatially like in Large Eddy Simulation (LES). In LES, the commutator of $\mathscr{C}$ and the filter is modelled

$$\partial_t \bar{u} + \mathscr{C}(\bar{u},\bar{u}) + \mathscr{D}(\bar{u}) + \nabla \bar{p} = \mathscr{C}(\bar{u},\bar{u}) - \overline{\mathscr{C}(u,u)} \approx \text{model}(\bar{u}), \tag{2}$$

where the filtered velocity is denoted by $\bar{u}$. Many of the regularly applied filters are isomorphisms [2]. Consequently, u and $\bar{u}$ have the same spectral support and the reduction of the computational complexity has to come from an alteration of the dynamics of $\bar{u}$, that is by taking the model in place of the commutator in Eq. (2) [3]. An appropriate model is hard to accomplish for a number of reasons. Carati et al. [4] have shown that the series expansion (in powers of the filter length) of the commutator in the right-hand side of (2) starts with a term that is known under various names, among others nonlinear model, gradient model and tensor-diffusivity model. This generic, leading-order term turns out to give rise to instabilities [5,6]. An approach based upon a truncated series expansion need be damped. The matter is complicated further if one insists that the mathematical structure of the closure model

* Tel.: +31 50 3633958; fax: +31 50 3933800.
E-mail address: R.W.C.P.Verstappen@rug.nl

0045-7930/$ - see front matter © 2007 Elsevier Ltd. All rights reserved.
doi:10.1016/j.compfluid.2007.01.013

is consistent with that of the underlying commutator (see [7], for example). In practice, closure models are often based on phenomenological arguments that cannot be derived formally from the Navier–Stokes equations. Today, a large number of models exists, see [8] and the references therein; Ref. [3] gives a recent review on mathematical issues related to the theory of LES.

To confine the dynamics, we need not alter the commutator in the filtered Navier–Stokes equations. Rather, we may alter the nonlinearity directly,

$$\partial_t u_\epsilon + \widetilde{\mathscr{C}}(u_\epsilon, u_\epsilon) + D(u_\epsilon) + \nabla p_\epsilon = 0, \tag{3}$$

where the variable name is changed from u to u_ϵ to stress that the solution of (3) differs from that of (1). In this paper, we will construct approximations $\widetilde{\mathscr{C}}$ of $\mathscr{C}$ with the help of a self-adjoint filter with length ϵ. In general, this filter need not be the same as the LES-filter in Eq. (2). To show that the approach given by Eq. (3) falls in with the concept of LES for any invertible LES-filter, we apply the LES-filter to Eq. (3) and compare the filtered equation term-by-term with (2) to identify the induced closure model:

$$\text{model}(\bar{u}) = \mathscr{C}(\bar{u}, \bar{u}) - \overline{\widetilde{\mathscr{C}}(u, u)}. \tag{4}$$

Eq. (4) relates $\widetilde{\mathscr{C}}(u,u)$ one-to-one to a closure model if the LES-filter is invertible.

The altered system (3) is more amenable to solve numerically, if the low modes of u_ϵ approximate the corresponding low modes of the Navier–Stokes solution u, and the high modes of u_ϵ vanish faster than those of u.

The first outstanding approach in this direction goes back to Leray [9], who filtered the transport velocity, $\widetilde{\mathscr{C}}(u,u) = \mathscr{C}(\bar{u},u)$, and proved that this yields a unique C^∞ solution for any filter length $\epsilon > 0$, which converges to the weak Navier–Stokes solution as $\epsilon \to 0$. Leray's proof ascertains that the energy cascade stops at a certain scale of motion, everywhere in the spatial domain and for all times. The spectrum of the Leray model consists of two parts. The usual Kolmogorov $|k|^{-5/3}$ law is found for short wave vectors k, whereas for small scales ($\epsilon|k| >> 1$) a much steeper $|k|^{-13/3}$ power law holds [10].

The Navier–Stokes-α model forms another example. In this example, the nonlinear term is written in rotational form, $\mathscr{C}_r(u,v) = (\nabla \times u) \times v$, and replaced by $\widetilde{\mathscr{C}}_r(u,u) = \mathscr{C}_r(u,\bar{u})$. The Navier–Stokes-α model may be derived in various ways [11–13]. Some of these derivations involve an averaging procedure that is partially performed in the Lagrangian framework. Therefore the equations are also known as the Lagrangian-averaged Navier–Stokes equations. The Navier–Stokes-α model has a unique solution in C^∞ (for any filter length $\epsilon > 0$), which converges to the weak Navier–Stokes solution as $\epsilon \to 0$. The energy spectrum follows the $|k|^{-5/3}$ law of Kolmogorov for $\epsilon|k| \ll 1$ and falls of like $|k|^{-3}$ for large k [14].

Basically, the nonlinearity is altered to restrain the convective energetic exchanges. In doing so, one can preserve certain fundamental properties of (the convective operator in) the Navier–Stokes equations, e.g., symmetries, conservation properties, transformation properties, Kelvin's circulation theorem, Bernoulli's theorem, Karman–Howarth's theorem, etc. [15]. In this paper, we propose to approximate the convective nonlinearity in such a manner that the symmetry properties that form the basis for the conservation of energy, enstrophy (in 2D) and helicity are preserved. The underlying idea is to restrain the convective production of small scales of motion, while ensuring that the solution does not blow up in the energy-norm (in 2D also: enstrophy-norm). This approach yields an unconditionally stable simulation method, provided the numerical approximation of $\widetilde{\mathscr{C}}$ preserves the symmetry properties too [16].

The paper is organized as follows. In Section 2, we recall the symmetry and conservation properties of turbulent convection. Symmetry-preserving approximations are introduced in Section 3. In Section 4, emphasis is given to the vortex stretching mechanism and triad interactions. The relationship with LES is elaborated in Section 5. Our choice of the filter and the numerical discretization are explained in Sections 6 and 7, respectively. The proposed simulation method is tested for turbulent channel flow in Section 8. The results are discussed in Section 9.

2. Symmetry and conservation properties

In terms of the usual scalar product $(u,v) = \int_V u \cdot v \, \mathrm{d}x$, the energy of a fluid occupying a region V is given by $|u|^2 = (u,u)$. The evolution of the energy follows from differentiating (u,u) with respect to time and rewriting $\partial_t u$ with the help of (1). In this way, we get a convective contribution given by $(\mathscr{C}(u,u),u)$.

The trilinear form $(\mathscr{C}(u,v),w)$ is skew-symmetric with respect to v and w,

$$(\mathscr{C}(u,v),w) = -(v,\mathscr{C}(u,w)), \tag{5}$$

provided $\int_{\partial V}(v\cdot w)(u\cdot n)\,\mathrm{d}s = 0$; e.g., if the normal velocity $u\cdot n$ vanishes at the boundary ∂V, if $v\cdot w$ vanishes, or if periodic boundary conditions apply. The proof of (5) uses the identity $\nabla\cdot(fu) = f\nabla\cdot u + \nabla f\cdot u$, which holds for any (differentiable) scalar f and vector field u. Taking $f = v\cdot w$, $\nabla\cdot u = 0$ and applying Gauß's Divergence Theorem gives $(\mathscr{C}(u,v)\cdot w) + (\mathscr{C}(u,w)\cdot v) = (\nabla f\cdot u) = (\nabla\cdot(fu)) = 0$, which proves (5).

Eq. (5) demonstrates that the convective contribution $(\mathscr{C}(u,u),u)$ cancels from the energy equation. The pressure does not contribute. Thus after some algebra, the energy equation reduces to

$$\frac{\mathrm{d}}{\mathrm{d}t}\frac{1}{2}|u|^2 = -\frac{1}{Re}|\nabla u|^2 = -\frac{1}{Re}|\nabla\times u|^2. \tag{6}$$

This shows that the enstrophy $|\nabla\times u|^2$ determines the rate of dissipation of energy.

The evolution of the enstrophy is obtained by projecting Eq. (1) on $-\Delta u$ [17]:

$$\frac{\mathrm{d}}{\mathrm{d}t}\frac{1}{2}|\nabla\times u|^2 = -\frac{1}{Re}|\Delta u|^2 - (\mathscr{C}(u,u),\Delta u). \tag{7}$$

In two spatial dimensions, we have

$$(\mathscr{C}(u,v),\Delta v) = (u,\mathscr{C}(\Delta v,v)), \tag{8}$$

see [18]. Taking $u=v$ and applying (5) yields $(\mathscr{C}(u,u),\Delta u)=0$, which shows that the enstrophy is conserved in 2D (if $\mathscr{D}=0$). This property is extensively used in the proof of the existence and uniqueness of (weak and strong) solutions of the 2D Navier–Stokes equations. In 3D, however, $(\mathscr{C}(u,u),\Delta u)\neq 0$ and the question of existence and uniqueness is still open. At the present level of understanding, it cannot be excluded that the vorticity,

$$\omega = \nabla\times u,$$

bursts driving the energy to extreme small scales by the vortex stretching mechanism.

The evolution of the helicity (ω,u) follows from the inner product of Eq. (1) with the vorticity ω and the inner product of the curl of Eq. (1),

$$\partial_t\omega + \mathscr{C}(u,\omega) + \mathscr{D}(\omega) = \mathscr{C}(\omega,u) \tag{9}$$

with the velocity u. Taking these inner products results into the convective contribution $(\mathscr{C}(u,u),\omega)+(\mathscr{C}(u,\omega),u)-(\mathscr{C}(\omega,u),u)$, which vanishes as an immediate consequence of the skew symmetry (5). Thus, the helicity is conserved (if $\mathscr{D}=0$).

3. Symmetry-preserving approximations

Approximations of particular interest conserve the energy, the enstrophy (in 2D) and the helicity (in 3D) in the absence of viscous dissipation. The Leray model conserves the energy, but not the enstrophy or helicity, whereas the Navier–Stokes-α model conserves the enstrophy and helicity, yet not the energy. Since the invariance of energy, enstrophy and helicity is intimately tied up with the symmetry properties of the convective operator $\mathscr{C}$ (see Section 2), we aim to approximate $\mathscr{C}$ in such manner that the symmetries given by Eqs. (5) and (8) are preserved. This criterion yields the following class of approximations:

$$\partial_t u_\epsilon + \mathscr{C}_n(u_\epsilon,u_\epsilon) + \mathscr{D}(u_\epsilon) + \nabla p_\epsilon = 0, \tag{10}$$

($n=2,4,6$) in which the convective term is approximated according to:

$$\mathscr{C}_2(u,v) = \overline{\mathscr{C}(\bar u,\bar v)} \tag{11}$$

$$\mathscr{C}_4(u,v) = \mathscr{C}(\bar u,\bar v) + \overline{\mathscr{C}(\bar u,v')} + \overline{\mathscr{C}(u',\bar v)} \tag{12}$$

$$\mathscr{C}_6(u,v) = \mathscr{C}(\bar u,\bar v) + \mathscr{C}(\bar u,v') + \mathscr{C}(u',\bar v) + \overline{\mathscr{C}(u',v')} \tag{13}$$

where a prime indicates the residual of the filter, e.g., $u' = u-\bar u$. Here it is worth noting that the convective operator $\mathscr{C}$ in the right-hand sides of (11)–(13) may also be written in rotational form.

The approximations $\mathscr{C}_n(u,v)$ of $\mathscr{C}(u,v)$ may be derived by smoothing the convective flux. For instance, $\mathscr{C}_4$ is found if $\int_{\partial W} vu\cdot n\,\mathrm{d}s$ is replaced by $\int_{\partial W}(\bar v\bar u + \overline{\bar v u'} + \overline{v'\bar u})\cdot n\,\mathrm{d}s$. The difference between $\mathscr{C}_n(u,v)$ and $\mathscr{C}(u,v)$ is of the order of ϵ^n with $n=2,4,6$, respectively (for a generic, symmetric filter). These orders follow straightforwardly from the observation that $u' = \mathscr{O}(\epsilon^2)u$ [4]. The Leray model and the Navier–Stokes-α model are second-order accurate.

The nonlinear approximations (11)–(13) are constructed in such a manner that the symmetry properties given by Eqs. (5) and (8) are preserved. That is, for any self-adjoint filter:

$$(\mathscr{C}_n(u,v),w) = -(v,\mathscr{C}_n(u,w)) \tag{14}$$

with $n=2,4,6$; and in 2D (provided the filter commutes with the Laplacian):

$$(\mathscr{C}_n(u,v),\Delta v) = (u,\mathscr{C}_n(\Delta v,v)). \tag{15}$$

To sketch the idea of the proof of Eqs. (14) and (15), we consider (14) for $n=4$. By definition of $\mathscr{C}_4$, we have

$$\begin{aligned}(\mathscr{C}_4(u,v),w) &= (\mathscr{C}(\bar u,\bar v) + \overline{\mathscr{C}(\bar u,v')} + \overline{\mathscr{C}(u',\bar v)},w)\\ &= (\mathscr{C}(\bar u,\bar v),w) + (\mathscr{C}(\bar u,v'),\bar w) + (\mathscr{C}(u',\bar v),\bar w),\end{aligned}$$

where we have used the self-adjointness of the filter, i.e., $(\bar u,v)=(u,\bar v)$. Moreover, we know that $\mathscr{C}$ is skew-symmetric, see Eq. (5); hence

$$\begin{aligned}(\mathscr{C}_4(u,v),w) &= -(\bar v,\mathscr{C}(\bar u,w)) - (v',\mathscr{C}(\bar u,\bar w)) - (\bar v,\mathscr{C}(u',\bar w))\\ &= -(v,\mathscr{C}(\bar u,\bar w)) - (v,\overline{\mathscr{C}(\bar u,w')}) - (v,\overline{\mathscr{C}(u',\bar w)})\\ &= -(v,\mathscr{C}_4(u,w)),\end{aligned}$$

which proves (14) for $n=4$.

Eq. (14) implies that the convective contribution to the energy equation vanishes. Consequently, the evolution of the energy $\frac{1}{2}|u_\epsilon^2|$ of any solution u_ϵ of (10)–(13) is again given by Eq. (6) with u replaced by u_ϵ.

The curl of (10) gives (provided the filter commutes with differentiation)

$$\partial_t\omega_\epsilon + \mathscr{C}_n(u_\epsilon,\omega_\epsilon) + \mathscr{D}(\omega_\epsilon) = \mathscr{C}_n(\omega_\epsilon,u_\epsilon), \tag{16}$$

where $n=2,4,6$. This evolution equation resembles the vorticity Eq. (9) that follows from the incompressible Navier–Stokes equations: the only difference is that $\mathscr{C}$ is replaced by the approximation $\mathscr{C}_n$. Now, as $\mathscr{C}$ and $\mathscr{C}_n$ possess the same symmetries, an argument similar to the one used to establish the conservation of enstrophy (in 2D) and helicity in Section 2, tells us that these invariances hold too in case the approximation $\mathscr{C}_n$ is applied.

Thus, the enstrophy of an inviscid flow governed by (10)–(13) is conserved in 2D, whereas in 3D the notorious high fluctuations of the trilinear form $(\mathscr{C}(u,u),\Delta u)$ in the enstrophy Eq. (7) are damped, by replacing $(\mathscr{C}(u,u),\Delta u)$ by $(\mathscr{C}_n(u_\epsilon,u_\epsilon),\Delta u_\epsilon)$, in the hope that this smoothing prevents the vorticity from bursting to small scales. The rigorous mathematical analysis of the regularity of the solution does not fall within the scope of the present paper. Perhaps, the analysis may be performed by means of the mathematical techniques that have been applied to prove the

regularity of Leray and Navier–Stokes-α solutions in [10,14], respectively.

Eq. (16) shows that vorticity is produced at the boundaries only. Furthermore, the symmetry (14) implies that Eq. (10) conserves a number of linear forms too (if $\mathscr{D}=0$). For instance, $(f(\omega_\epsilon),1)$ is conserved for any scalar function f with ∇f constant.

3.1. Pressure

By taking the divergence of the Navier–Stokes equations, in an incompressible fluid, we find the following Poisson equation for the pressure:

$$\Delta p=\frac{1}{2}\omega^2(u)-\frac{1}{2}\sigma^2(u),$$

where $\omega^2(u)=\frac{1}{2}(\partial_i u_j-\partial_j u_i)^2$ and $\sigma^2(u)=\frac{1}{2}(\partial_i u_j+\partial_j u_i)^2$, see [19], e.g., This equation establishes an analogy to electrostatics, with the pressure corresponding to the potential resulting from negative and positive charges distributed in proportion to $\frac{1}{2}\omega^2$ and $\frac{1}{2}\sigma^2$, respectively. By taking the divergence of Eq. (10), we get

$$\begin{aligned}
\Delta p_\epsilon &= \overline{\frac{1}{2}\omega^2(\bar{u}_\epsilon)-\frac{1}{2}\sigma^2(\bar{u}_\epsilon)},\\
\Delta p_\epsilon &= \overline{\frac{1}{2}\omega^2(u_\epsilon)-\frac{1}{2}\sigma^2(u_\epsilon)}+\left(\frac{1}{2}\omega^2(\bar{u}_\epsilon)-\frac{1}{2}\sigma^2(\bar{u}_\epsilon)\right)'\\
&\quad-\overline{\frac{1}{2}\omega^2(u'_\epsilon)-\frac{1}{2}\sigma^2(u'_\epsilon)},\\
\Delta p_\epsilon &= \frac{1}{2}\omega^2(u_\epsilon)-\frac{1}{2}\sigma^2(u_\epsilon)-\left(\frac{1}{2}\omega^2(u'_\epsilon)-\frac{1}{2}\sigma^2(u'_\epsilon)\right)'
\end{aligned}$$

for $n=2,4,6$, respectively (provided the filter commutes with the divergence operator). In conclusion, the approximations $\mathscr{C}_n$ of the nonlinearity $\mathscr{C}$ result into a smoother distribution of the ω^2 and σ^2 charges, that is lead to a smoother right-hand side of the Poisson equation for the pressure and thus smooth the pressure.

Because the approximations given by (11)–(13) make no distinction between the transport velocity and the actual fluid velocity, we can easily generalize Bernoulli's theorem. As an example, we consider the approximate model $\mathscr{C}_4$. In this case, Bernoulli's theorem changes from its well-known form to: in a stationary ($\partial_t u=0$), inviscid ($\mathscr{D}=0$) flow governed by (10) + (12) the quantity

$$\frac{1}{2}\overline{|u_\epsilon|^2}+\frac{1}{2}(|\bar{u}_\epsilon|^2)'-\frac{1}{2}\overline{|u'_\epsilon|^2}+p_\epsilon$$

is constant along any curve parameterized by $r(t)$ where the tangential vector satisfies

$$\dot{r}\perp\overline{(\nabla\times u_\epsilon)\times u_\epsilon}+((\nabla\times\bar{u}_\epsilon)\times\bar{u}_\epsilon)'-\overline{(\nabla\times u'_\epsilon)\times u'_\epsilon}.$$

The proof uses the same lines of reasoning as the proof of Bernoulli's theorem in [20] and is therefore omitted here. In conclusion, Eqs. (10)–(13) are not only conservative, but also allow for the definition of smooth streamlines along which a smooth form of $\frac{1}{2}|u|^2+p$ is transported.

4. Production of small scales

To see how the approximations given by (11)–(13) restrain the production of small scales of motion, we consider the vortex stretching and triad interactions, respectively.

4.1. Vortex stretching mechanism

If it happens that the source term $\mathscr{C}_n(\omega_\epsilon,u_\epsilon)$ in Eq. (16) is so strong that the dissipative term $\mathscr{D}(\omega_\epsilon)$ cannot prevent the intensification of vorticity, smaller and smaller vortical structures may be produced locally. The Navier–Stokes equations lead to the source term

$$\mathscr{C}(\omega,u)=S(u)\omega, \tag{17}$$

where $S(u)=\frac{1}{2}(\nabla u+\nabla u^{\mathrm{T}})$ is the deformation tensor. The trace of this symmetric tensor is zero. Consequently, $S(u)$ has at least one non-negative eigenvalue. If ω is aligned with an eigenvector associated with a positive eigenvalue, then the source term $\mathscr{C}(\omega,u)$ in Eq. (9) is positive, which may lead to an increase of the vorticity magnitude. As the angular momentum is conserved (in the absence of viscous dissipation) an increase of the vorticity magnitude implies that fluid elements are stretched along the direction of the eigenvector associated with the positive eigenvalue. This phenomenon, called vortex stretching, implies a transfer of energy from large scales of motion to smaller ones, i.e., drives the energy cascade. Here, it may be noted that the evolution of a short material line element δr is given by $\partial_t\delta r+\mathscr{C}(u,\delta r)=\mathscr{C}(\delta r,u)$. Thus it is as if the vorticity behaves like a line material element coinciding instantaneously with a portion of the vortex line. The source in the dynamics of $|\delta r|^2$ is given by $\mathscr{C}(\delta r,u)\cdot\delta r=\delta r\cdot\mathscr{S}(u)\delta r$.

The approximations (11)–(13) alter the vortex stretching mechanism in 3D ($\mathscr{C}_n(\omega_\epsilon,u_\epsilon)$ is identically zero in 2D). The vortex stretching term becomes:

$$\mathscr{C}_2(\omega,u)=\overline{\bar{S}\bar{\omega}}, \tag{18}$$

$$\mathscr{C}_4(\omega,u)=\overline{S}\bar{\omega}+\overline{\bar{S}\omega'}+\overline{S'\bar{\omega}}, \tag{19}$$

$$\mathscr{C}_6(\omega,u)=\overline{S}\bar{\omega}+\overline{S}\omega'+S'\bar{\omega}+\overline{S'\omega'}. \tag{20}$$

In the Navier–Stokes dynamics, vortex stretching leads to the production of smaller and smaller scales; hence to a continuous, local increase of both S' and ω'. Consequently, at the positions where vortex stretching occurs, the terms with S' and ω' will eventually amount considerably to $S\omega=\overline{S}\overline{\omega}+\overline{S}\omega'+S'\bar{\omega}+S'\omega'$. Since these terms are diminished in (18)–(20), the symmetry-preserving approximations $\mathscr{C}_n$ of the convective term counteract the production of smaller and smaller scales by means of vortex stretching and may eventually stop the continuation of the vortex stretching process.

4.2. Triadic interactions

To study the interscale interactions in more detail, we continue in the spectral space. The spectral representation of the convective term in the Navier–Stokes equations is given by

$$\mathscr{C}_k(\hat{u},\hat{v}) = \mathrm{i}\Pi(k)\sum_{p+q=k}\hat{u}_p q\hat{v}_q, \tag{21}$$

where $\Pi(k) = I - k\ k^{\mathrm{T}}/|k|^2$ denotes the projector onto divergence-free velocity fields in the spectral space. Taking the Fourier transform of (10)–(13), we obtain the evolution of each Fourier-mode $\hat{u}_k(t)$ of u_ϵ for the approximation $\mathscr{C}_n$:

$$\left(\frac{\mathrm{d}}{\mathrm{d}t} + \frac{|k|^2}{Re}\right)\hat{u}_k + \mathrm{i}\Pi(k)\sum_{p+q=k} f_n(\hat{g}_k,\hat{g}_p,\hat{g}_q)\hat{u}_p q\hat{v}_q = 0. \tag{22}$$

The mode $\hat{u}_k(t)$ interacts only with those modes whose wave vectors p and q form a triangle with the vector k. Compared with (21), every triad interaction is multiplied by

$$\begin{aligned} f_2(\hat{g}_k,\hat{g}_p,\hat{g}_q) &= \hat{g}_k\hat{g}_p\hat{g}_q,\\ f_4(\hat{g}_k,\hat{g}_p,\hat{g}_q) &= \hat{g}_k\hat{g}_p + \hat{g}_k\hat{g}_q + \hat{g}_p\hat{g}_q - 2\hat{g}_k\hat{g}_p\hat{g}_q,\\ f_6(\hat{g}_k,\hat{g}_p,\hat{g}_q) &= 1-(1-\hat{g}_k)(1-\hat{g}_p)(1-\hat{g}_q), \end{aligned}$$

where $\hat{g}_k$ denotes the kth Fourier-mode of the kernel of the convolution filter, i.e., $\overline{\hat{u}}_k = \hat{g}_k\hat{u}_k$. The functions f_n satisfy $f_n(1,1,1) = 1$ and $f_n(0,0,0) = 0$. Furthermore, all the first-order partial derivatives of $f_n(\hat{g}_k,\hat{g}_p,\hat{g}_q)$ are strictly positive for $0 < \hat{g}_k,\hat{g}_p,\ \hat{g}_q < 1$. Hence, the factor $f_n(\hat{g}_k,\hat{g}_p,\hat{g}_q)$ by which every Navier–Stokes interaction is multiplied is a monotone function of $\hat{g}_k,\ \hat{g}_p$, and $\hat{g}_q$.

A generic, symmetric convolution filter satisfies

$$\hat{g}_k = 1 - \alpha^2|k|^2 + \mathscr{O}(\alpha^4) \quad \text{with } \alpha^2 = \epsilon^2/24,$$

see for instance [4]. Consequently,

$$\begin{aligned} f_2 &\approx 1 - \alpha^2(|k|^2 + |p|^2 + |q|^2),\\ f_4 &\approx 1 - \alpha^4(|k|^2|p|^2 + |k|^2|q|^2 + |p|^2|q|^2),\\ f_6 &\approx 1 - \alpha^6|k|^2|p|^2|q|^2, \end{aligned}$$

respectively. In other words, the interactions between large scales of motion (short wave vectors) approximate the Navier–Stokes dynamics up to $\mathscr{O}(\epsilon^n)$, with $n = 2,4,6$, respectively.

In order to investigate interactions involving longer wave vectors (smaller scales), the filter need be specified further. To that end, we consider the Helmholtz filter:

$$\hat{g}_k = \frac{1}{1+\alpha^2|k|^2}.$$

Here we will restrict ourselves to the approximation $\mathscr{C}_4$; a similar analysis may be performed for $\mathscr{C}_2$ and $\mathscr{C}_6$. In case a Helmholtz filter is applied, the spectral representation of the approximation $\mathscr{C}_4$ becomes

$$\mathrm{i}\Pi(k)\sum_{p+q=k}\hat{u}_p q\hat{u}_q\frac{1+\alpha^2(|k|^2+|p|^2+|q|^2)}{(1+\alpha^2|k|^2)(1+\alpha^2|p|^2)(1+\alpha^2|q|^2)}.$$

By comparing this expression with Eq. (21), we see that all contributions to the sum are reduced. The amount by which the interactions are lessened depends on the length of the legs of the triangle $k = p + q$. The reduction is the largest for triangles with three long legs, i.e., $\alpha^2|k|^2 \gg 1$, $\alpha^2|p|^2 \gg 1$ and $\alpha^2|q|^2 \gg 1$. For those triangles, the Navier–Stokes interaction is multiplied by

$$f_4 \approx \frac{1}{\alpha^4|k|^2|p|^2} + \frac{1}{\alpha^4|k|^2|q|^2} + \frac{1}{\alpha^4|p|^2|q|^2}.$$

The non-local interactions between a large scale characterized by $\alpha^2|k|^2 \ll 1$ and two small scales satisfying $\alpha^2|p|^2 \gg 1$ and $\alpha^2|q|^2 \gg 1$ are multiplied by

$$f_4 \approx \frac{1}{\alpha^2|p|^2} + \frac{1}{\alpha^2|q|^2}.$$

In general, we see that with a Helmholtz filter the approximation $\mathscr{C}_4$ (strongly) attenuates all interactions for which at least two legs of the triangle $k = p + q$ are (much) longer than $1/\alpha$, whereas all possible triadic interactions for which at least two legs are (much) shorter than $1/\alpha$ are reduced to a small degree. Since in the latter case the longest leg is always shorter than $2/\alpha$, we may conclude that the approximation $\mathscr{C}_4$ confines the dynamics for the greatest part to scales whose wavevector-length is smaller than $2/\alpha$. In this way, the resolution requirements resulting from the convective nonlinearity are reduced.

5. Relation to LES

Eq. (4) relates the approximations given by Eqs. (11)–(13) one-to-one to LES-models if the filter is invertible. In this section, this relationship will be elaborated for approximate deconvolution models as well as for the (nonlinear) gradient model.

5.1. Approximate deconvolution

The approximations $\mathscr{C}_n$ may be seen in relationship to the approximate deconvolution method (ADM). Stolz and Adams [21] proposed to replace the argument u of $\overline{\mathscr{C}(u,u)}$ by the following approximate deconvolution of the filtered velocity field: $\widetilde{u} = \widetilde{\mathscr{F}}^{-1}\bar{u} \approx u$, where $\widetilde{\mathscr{F}}^{-1}$ approximates the inverse of the filter $\mathscr{F}u = \bar{u}$. They constructed an approximate inverse by truncating the formal series expansion of the inverse. To illustrate our choice, we note that the evolution of the approximately deconvolved velocity,

$$\partial_t\tilde{u} + \widetilde{\mathscr{F}}^{-1}\mathscr{F}\mathscr{C}(\tilde{u},\tilde{u}) + \mathscr{D}(\tilde{u}) + \nabla\tilde{p} = 0,$$

equals Eq. (3) if we take $\tilde{u} = u_\epsilon, \tilde{p} = p_\epsilon$ and $\widetilde{\mathscr{C}}(u,v) = \widetilde{\mathscr{F}}^{-1}\mathscr{F}\mathscr{C}(u,v)$. Thus, it is mathematically evident that any direct modification of the convective term in the

Navier–Stokes equations is implicitly related to an approximate deconvolution operator $\widetilde{\mathscr{F}}^{-1}$. From a physical point of view, however, not all, but only some modifications constitute a proper, approximate model. The modification $\mathscr{C}_n(u,v)$ of $\mathscr{C}(u,v)$ defines the approximate deconvolution operator implicitly by means of

$$\widetilde{\mathscr{F}}_n^{-1}\mathscr{F}\mathscr{C}(u,v) = \mathscr{C}(u,v) + \mathscr{E}_n(u,v),$$

where the error in the approximation is given by $\mathscr{E}_n(u,v) = \mathscr{C}_n(u,v) - \mathscr{C}(u,v)$. This error is $\mathscr{O}(\epsilon^n)$ for any symmetric filter (with filter length ϵ), and $\mathscr{E}_n$ preserves the symmetries given by Eqs. (5) and (8), which marks our approach.

5.2. Relation to (nonlinear) gradient model

Carati et al. [4] have shown that (for all symmetric filters that are C^∞ in wave space) the series expansion of the commutator of the convective operator $\mathscr{C}$ and the spatial filter is given by

$$\mathscr{C}(\bar{u}_\epsilon,\bar{u}_\epsilon) - \overline{\mathscr{C}(u_\epsilon,u_\epsilon)} = -\frac{1}{12}\epsilon^2 \mathrm{div}(\nabla\bar{u}_\epsilon\cdot\nabla\bar{u}_\epsilon) + \mathscr{O}(\epsilon^4), \quad (23)$$

provided the (filtered) velocity can be differentiated sufficiently often. The generic, second-order term in the right-hand side is referred to as (nonlinear) gradient model or tensor diffusivity model [22,23]. Leonard [6] has applied the gradient model to the scalar advection–diffusion equation for the filtered scalar $\bar{\phi}$:

$$\partial_t\bar{\phi} + \mathscr{C}(\bar{u},\bar{\phi}) + \mathscr{D}(\bar{\phi}) = -\frac{1}{12}\epsilon^2\overline{S}_{ij}\partial_i\partial_j\bar{\phi}, \quad (24)$$

where $\overline{S} = \frac{1}{2}(\nabla\bar{u} + \nabla\bar{u}^T)$ can be seen as a tensorial viscosity with both positive and negative eigenvalues. In the directions associated with the positive eigenvalues of $\overline{S}$, the right-hand side in (24) counteracts the viscous term $\mathscr{D}(\bar{\phi})$. Therefore, the gradient model need be stabilized in this application. The stability of the gradient model has also been analyzed with the help of the one-dimensional Burgers' equation by Vreman [5]. He showed that the gradient model gives rise to severe instabilities too. In Ref. [22] it is shown that the gradient model leads to a globally stable LES if the skewness of $\bar{u}$ is negative. Then, the direction(s) of negative diffusion continuously change so that the simulation remains globally stable. But the gradient model does not dissipate sufficient energy. In the original form of Clark et al. [23], this was overcome by combining the gradient model with an eddy-viscosity model, i.e., by adding a dissipative $\mathscr{O}(\epsilon^2)$-term. This mix effectively stabilizes the gradient model [5].

The approximations $\mathscr{C}_n$ can be related to closure models with the help of Eq. (4). From $\mathscr{C}_n(u_\epsilon,u_\epsilon) = \mathscr{C}(u_\epsilon,u_\epsilon) + \mathscr{O}(\epsilon^n)$ and Eq. (23), we obtain

$$\mathrm{model}(\bar{u}_\epsilon) = -\frac{1}{12}\epsilon^2\mathrm{div}(\nabla\bar{u}_\epsilon\cdot\nabla\bar{u}_\epsilon) + \mathscr{O}(\epsilon^4,\epsilon^n).$$

Thus, the gradient model forms the leading-order term of the closure models resulting from the fourth- and sixth-order approximations $\mathscr{C}_4$ and $\mathscr{C}_6$. Since both $\mathscr{C}_4$ and $\mathscr{C}_6$ are unconditionally stable (in the energy-norm), we can see them as higher-order, anisotropic stabilizations of the gradient model. The second-order approximation $\mathscr{C}_2$ adds $-\frac{1}{12}\epsilon^2\Delta\mathscr{C}(\bar{u}_\epsilon,\bar{u}_\epsilon) + \mathscr{O}(\epsilon^4)$ to the gradient model.

6. Choice of the filter

Filtering is usually done by means of an integral operator with a symmetrical convolution kernel. The subset of differential filters is obtained when the convolution kernel is taken equal to the Green's function associated with the inverse of a linear differential operator. Our filter is based on the elliptic differential operator

$$(1 - \alpha_i^2\partial_{ii}^2)\bar{u} = u, \quad (25)$$

where the coefficients α_1, α_2 and α_3 parameterize the length of the filter in the x_1-, x_2- and x_3-direction, respectively. Eq. (25) reduces to the Helmholtz filter in the isotropic case: $\alpha_i = \alpha$. The filter given by (25) is generic in the sense that any symmetric convolution filter can be approximated by the diffusive process (25), where the error in the approximation is of the order α_i^4 [4]. The boundary conditions that supplement the Navier–Stokes equations are applied to (25) too.

The elliptic filter (25) and the diffusive term in the Navier–Stokes equations are discretized in an identical manner, see [16] for details. This results into the following linear set of equations for the discrete filtered velocity $\bar{u}_h$:

$$F\bar{u}_h = u_h. \quad (26)$$

Solving this set of equations is rather expensive, more so because in the present application the filter merely functions as a smoothing operator. For that reason, we do not fully solve Eq. (26), but choose to perform just one Jacobi iteration with $\bar{u}_h = u_h$ as initial guess:

$$\mathrm{diag}(F)\bar{u}_h = (\mathrm{diag}(F) - F + I)u_h. \quad (27)$$

The unknown $\bar{u}_h$ can always be solved from this equation, since the entries of $\mathrm{diag}(F)$ are strictly positive (by definition). Moreover, the linear map $u_h \mapsto \bar{u}_h$ defined by Eq. (27) possesses the following two basic properties. I. A constant velocity vector is unaffected, that is Eq. (27) yields $\bar{1} = 1$, since $F1 = 1$; II. The operator in the right-hand side of (27) reduces the high-frequency components of the discrete velocity vector u_h (by construction). This mean that Eq. (27) constitutes a suitable filter for our application. To illustrate it, we consider a uniform, one-dimensional grid with spacing h. When we apply a second-order, central discretization, for example, Eq. (27) becomes

$$(1 + 2a^2)\bar{u}_i = a^2u_{i-1} + u_i + a^2u_{i+1}$$

with $a = \alpha/h$. The choice $a = 1$, e.g., leads to a box filter.

7. Numerical approximation

The discretization of Eq. (10) is an important point, since modelling errors and discretization errors are mixed together if results computed with the help of (10) are compared with reference data. The approximations $\mathscr{C}_n$ of $\mathscr{C}$ are constructed such that the properties given by Eqs. (5) and (8) are preserved. Of course, the same should hold for the spatial discretization of $\mathscr{C}_n$. Therefore, we have developed a discretization scheme that preserves Eqs. (5) and (8). In short (for a detailed explanation see [16]), the temporal evolution of the spatially discrete velocity vector $u_h(t)$ is governed by the following fourth-order, finite-volume discretization of Eq. (10):

$$\Omega \frac{\mathrm{d}u_h}{\mathrm{d}t} + C_n(u_h)u_h + Du_h - M^{\mathrm{T}}p_h = 0, \tag{28}$$

where the discrete incompressibility constraint reads $Mu_h = 0$. The diffusive matrix D is symmetric and positive semi-definite; it represents the integral of the diffusive flux $-\nabla u \cdot n/Re$ over the surfaces of the control volumes. The diagonal matrix Ω describes the sizes of the control volumes. The approximate, convective flux is discretized as in [16]. The resulting convective matrix $C_n(u_h)$ is skew-symmetric

$$C_n(u_h) + C_n^{\mathrm{T}}(u_h) = 0, \tag{29}$$

and satisfies the enstrophy-invariance discretely (in 2D). Eq. (29) forms the discrete analogue of Eq. (14). In a discrete setting, the skew symmetry (29) implies that

$$C_n(u_h)v_h \cdot w_h = v_h \cdot C_n^{\mathrm{T}}(u_h)w_h \overset{(29)}{=} -v_h \cdot C_n(u_h)w_h$$

for all discrete velocity vectors u_h, v_h and w_h. In our discrete context, the scalar product $(u, v) = \int_V u \cdot v \, \mathrm{d}x$ of two continuous functions u and v is approximated by $(u_h, v_h)_h = u_h \cdot \Omega v_h$. That is, the numerical integration of $\int_V u \cdot v \, \mathrm{d}x$ is done with the help of the rule that was used for the finite-volume integration of the time-derivative in (28). The evolution of the discrete energy $\|u_h\|_h^2 = u_h \cdot \Omega u_h$ of any solution u_h of Eq. (28) is then governed by the inequality

$$\frac{\mathrm{d}}{\mathrm{d}t}||u_h||_h^2 = -u_h \cdot (D + D^{\mathrm{T}})u_h \leqslant 0, \tag{30}$$

where the convective contribution cancels because of (29); compare the discretization of the energy equation given by (30) with the continuous expression (6). Note that the rate of change of energy is neither influenced by pressure differences since $Mu_h = 0$. The inequality (30) shows that the discrete energy does not increase; hence the symmetry-preserving, spatial discretization (28) is stable on any grid. Consequently, the choice of the grid may be based on the required accuracy solely and the main question becomes: how accurate is the simulation model?

8. Results for channel flow

As a first step in application of the symmetry-preserving approximations, the approximation $\mathscr{C}_4$ is tested for a turbulent channel flow by means of a comparison with the direct numerical simulations (Re_τ=180 and Re_τ=395). This flow forms a prototype for near-wall turbulence: virtually every LES has been tested for it. We consider two, coarse, computational grids consisting of $16 \times 16 \times 8$ and $32 \times 32 \times 16$ grid points, respectively. Details about the numerics (grid-stretching, time-stepping, etc.) can be found in [16]. The results will be compared to the DNS data of Kim et al. [24] at $Re_\tau = 180$; for $Re_\tau = 395$, we will use the DNS data of Moser et al. [25] for comparison. The extend of the computational domain in the periodical directions is identical with that of the DNS's in Ref. [24,25], respectively.

In the present test, the coefficients α_i of the elliptic differential filter (25) are taken such that the corresponding length $\epsilon_i = \alpha_i\sqrt{24}$ of the filter in the ith spatial direction becomes equal to $\epsilon_i = r\ h_i$, where the parameter r does not dependent on the coordinate direction and h_i denotes the average grid width in x_i. Consequently, the approximation $\mathscr{C}_4$ contains one parameter only, the ratio r of the filter length ϵ_i to the average grid width h_i. Since this ratio is chosen identical in all directions, we will write ϵ/h rather than ϵ_i/h_i, for convenience.

The least to be expected from numerical simulations of turbulence is a good prediction of the mean flow. Figs. 1 and 2 show that the symmetry-preserving approximation $\mathscr{C}_4$ satisfies that minimal requirement already at very coarse grids: $16 \times 16 \times 8$ grid points for $Re_\tau = 180$ and $32 \times 32 \times 16$ for $Re_\tau = 395$, respectively (for $2 < \epsilon/h < 4$). In both cases, the grid is chosen such that the first discrete streamwise velocity lies at $y^+ \approx 3$. The next is located at $y^+ \approx 10$.

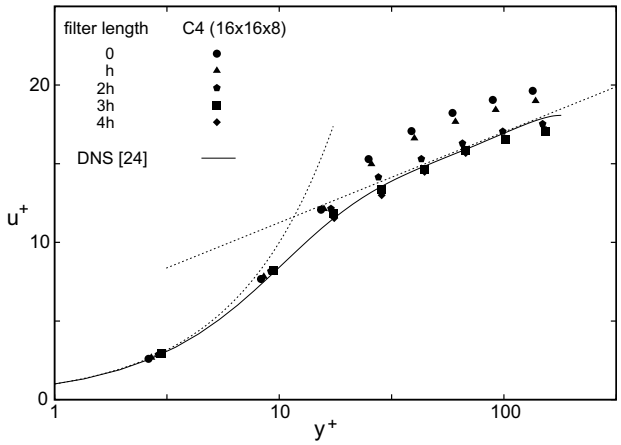

Fig. 1. The mean velocity (in wall coordinates) as obtained from the $16 \times 16 \times 8$ simulations at $Re_\tau = 180$. The ratio ϵ/h (filter length to the grid width) varies from zero to four. The symbols correspond to the numerical data at the grid points. The line represents the results of the DNS by Kim et al. [24].

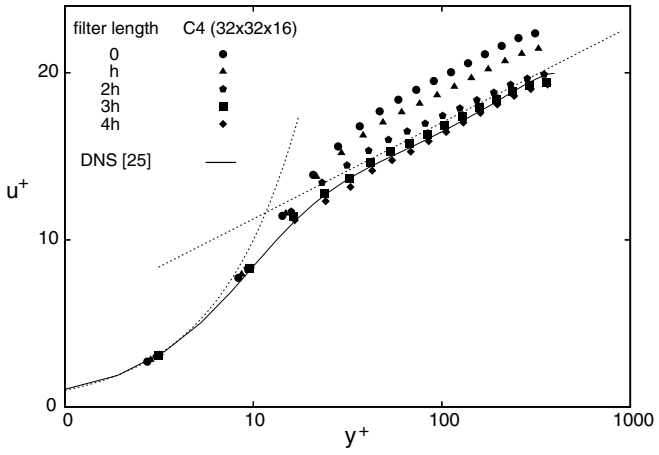

Fig. 2. Idem, $32 \times 32 \times 16$ grid points and $Re_\tau = 395$. The line represents the DNS data of Moser et al. [25].

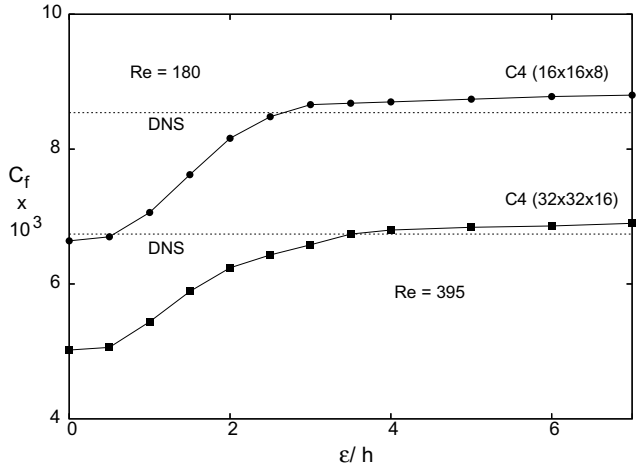

Fig. 3. Convergence of the skin friction as function of the filter-length for $Re_\tau = 180$ (upper curve) and $Re_\tau = 395$.

The location of the other points can be observed too: each symbol in Figs. 1 and 2 corresponds to a point of the grid.

Fig. 3 illustrates the convergence of the skin friction coefficient as function of the ratio ϵ/h (filter length to grid width). Here, the reference values are depicted by the dashed line. Overall good agreement between the $\mathscr{C}_4$-calculation at the $32 \times 32 \times 16$ grid and the DNS by Kim et al. [24] is observed for both the first- and second-order statistics, see Fig. 4. Fig. 5 shows a comparison of the velocity fluctuations with the DNS by Moser et al. [25] at $Re_\tau = 395$.

Our approach is based on the idea that the low modes of the solution u_ϵ of Eq. (10) approximate the corresponding low modes of the solution u of the Navier–Stokes equations, whereas the high modes of u_ϵ vanish faster than those of u. In order to investigate this basic idea, we consider the one-dimensional, streamwise energy spectra at $y^+ \approx 3$, i.e. at the first point of the $16 \times 16 \times 8$ grid (counted from the wall) and at $y^+ \approx 180$ i.e. in the center of the channel ($Re_\tau = 180$) Fig. 6 (upper graph) displays the near-wall

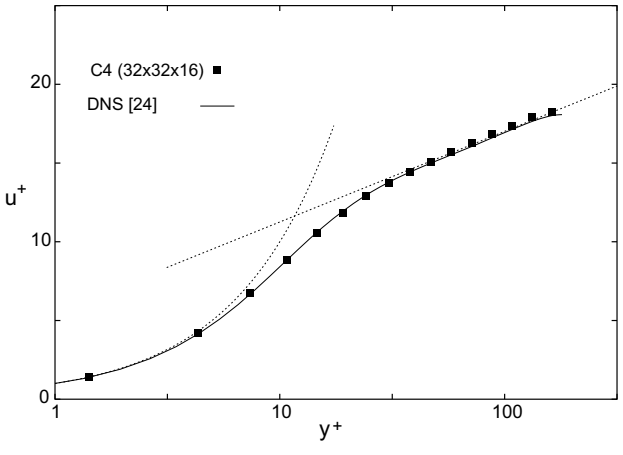

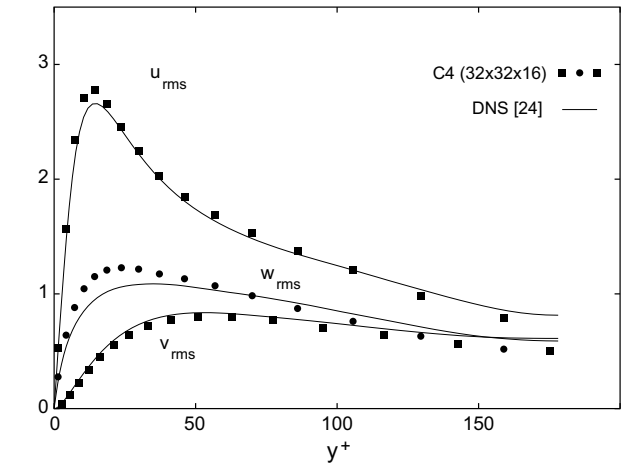

Fig. 4. Mean velocity and root-mean-square velocity fluctuations of the $32 \times 32 \times 16$ simulation for $\epsilon/h = 1.5$ and $Re_\tau = 180$.

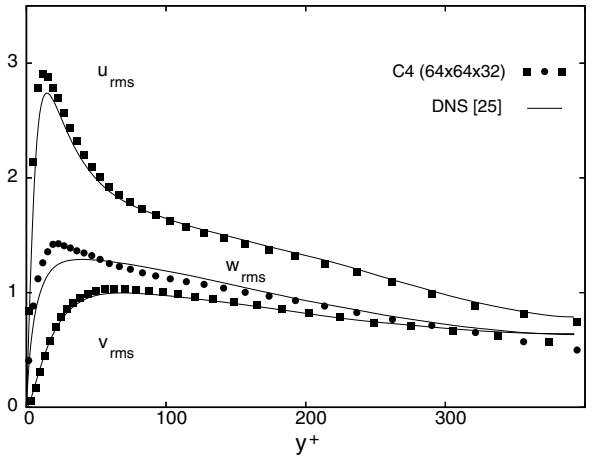

Fig. 5. Root-mean-square velocity fluctuations of the $64 \times 64 \times 32$ simulation for $\epsilon/h = 2$ and $Re_\tau = 395$.

energy spectra as obtained for $16 \times 16 \times 8$ grid points without ($\epsilon = 0$) and with modification ($\epsilon/h = 3$). Without any modification of the convective term, all modes (including the zeroth) in the energy spectrum differ from the reference spectrum. Here, the reference is taken from a DNS (identi-

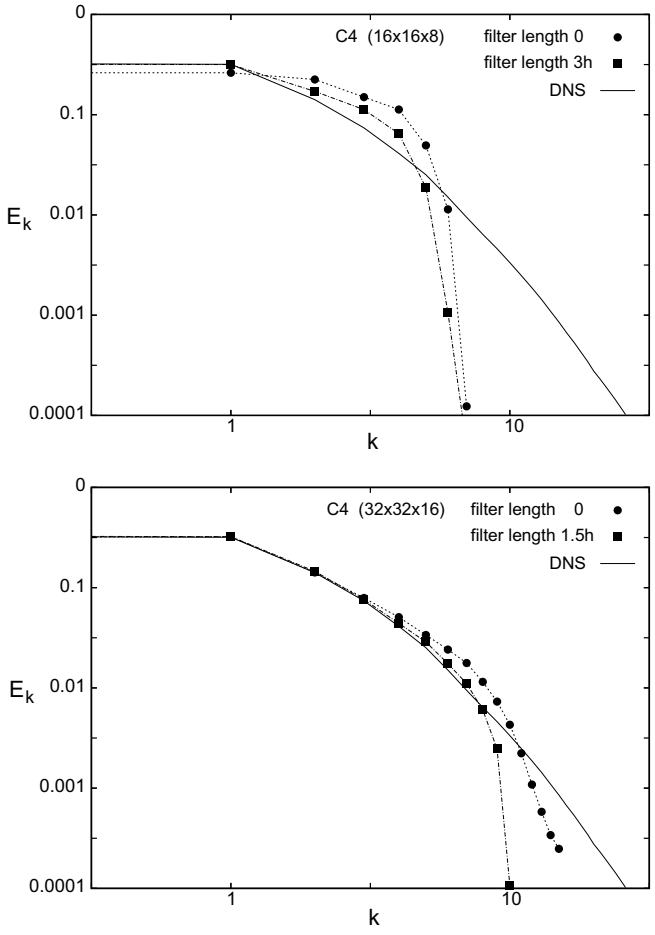

Fig. 6. One-dimensional (streamwise) energy spectra at $y^+ \approx 3$ ($Re_\tau = 180$).

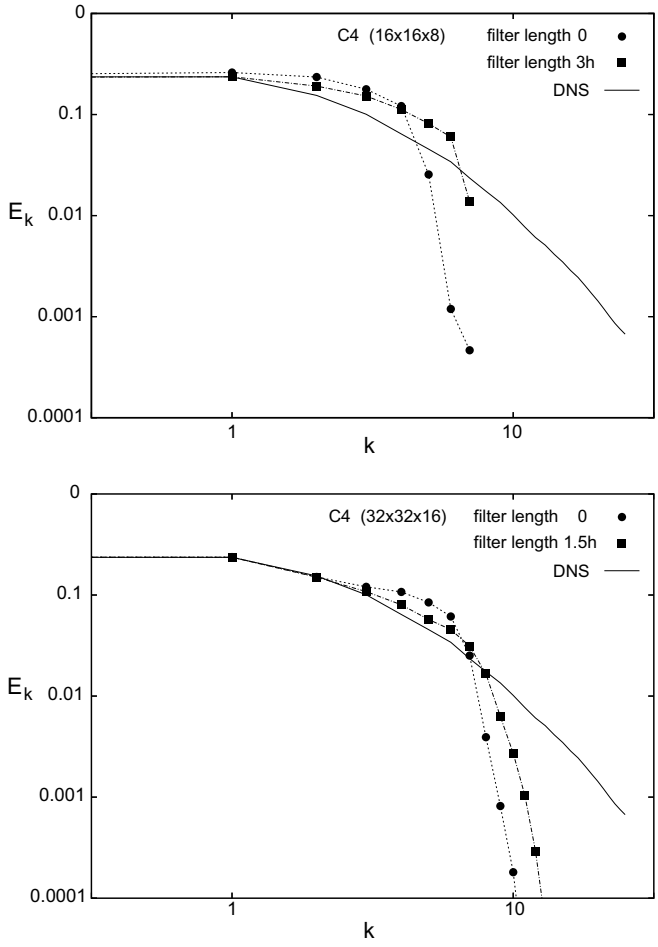

Fig. 7. One-dimensional (streamwise) energy spectra at $y^+ \approx 180$ ($Re_\tau = 180$).

cal numerical method, $128 \times 128 \times 64$ grid points, see [16] for details). With the modification $\mathscr{C}_4$ (and $\epsilon/h = 3$) the head of the energy spectrum improves significantly: the zeroth and first mode agree well with the DNS and the error in the modes two to five reduces strongly. Fig. 6 (lower graph) depicts essentially the same for the finer $32 \times 32 \times 16$ grid: the energy spectrum of the solution of (10) + (12) follows the DNS for large scales of motion, whereas a much steeper (numerically speaking: more gentle) power law is found for smaller scales. Fig. 7 focusses on the spectral behavior away from the boundaries. Again, the leading modes of the energy spectrum improve significantly if the modification $\mathscr{C}_4$ is applied. Yet, the agreement with the DNS is somewhat less in the center of the channel than near the wall. In summary, Figs. 6 and 7 illustrate the potential of the present approach: it improves the leading modes, whereas the tail vanishes fast, which is precisely what a simulation shortcut is ought to do.

9. Discussion and future research

The nonlinear term $\mathscr{C}_4(u_\epsilon, u_\epsilon)$ in Eq. (10) redistributes the energy among the various scales of motion, without affecting the total amount of energy. The production of small scales of motion is regulated by means of a gradual reduction of the flux of energy through the high wave numbers. As an inevitable result, however, the intermediate scales (i.e., the scales just before the point at which the spectrum falls off sharply) possess too much energy, because they cannot transport sufficient energy to the small scales. Figs. 6 and 7 provide an illustration hereof. The approach need be refined further by adding a model that dissipates the overshoot of energy in the intermediate scales. This may be a (dynamic) Smagorinsky-type model. Here, we propose another approach that is based on the group of invariant (space- and time-)transformations of the Navier–Stokes equations. A transformation $\mathscr{T}$ is said to be an invariant transformation if for all solutions u of the Navier–Stokes equations, $\mathscr{T}u$ is also a solution. These transformations are listed in Ref. [26], for instance. The approximation $\mathscr{C}_4$ maintains all invariant transformations of the Navier–Stokes equations, except the Galilean transformation $\mathscr{T}u(x,t) = u(x - a(t), t) - \ddot{a}(t)$, where $a(t)$ denotes an arbitrary, twice differentiable, function of time; the pressure $p(x,t)$ transforms into $p(x - a(t),\ t) - x \cdot \ddot{a}$. The Galilean invariance follows from the observation that

if we substitute $\mathscr{T}u$ for u in Eq. (1), there is a cancellation of terms between $\partial_t u$ and $\mathscr{C}(u,u)$. In general, however, this will not be the case if $\mathscr{C}(u,u)$ is replaced by $\widetilde{\mathscr{C}}(u,u)$. Therefore, we propose to modified the time-derivative,

$$\tilde{\partial}_t u_\epsilon + \widetilde{\mathscr{C}}(u_\epsilon, u_\epsilon) + \mathscr{D}(u_\epsilon) + \nabla p_\epsilon = 0,$$

in such a way that the Galilean invariance is preserved. In case $\widetilde{\mathscr{C}}(u_\epsilon, u_\epsilon) = \mathscr{C}_4(u_\epsilon, u_\epsilon)$, the Galilean invariance is restored if we replace the time-derivative $\partial_t u_\epsilon$ by the following fourth-order approximation:

$$\tilde{\partial}_t u_\epsilon = \partial_t (u_\epsilon - u''_\epsilon),$$

where $u'' = u' - \overline{u'}$. This modification shortens the characteristic turnover time of the smallest eddies in the flow. In other words, it fortifies the enstrophy of the smallest scales of motion and thus it constitutes a dissipation model. The energy equation becomes

$$\frac{\mathrm{d}}{\mathrm{d}t}\frac{1}{2}(|u_\epsilon|^2 - |u'_\epsilon|^2) = -\frac{1}{Re}|\nabla u_\epsilon|^2,$$

provided the filter is self-adjoint. The analysis of this dissipation model is part of our future research plans.

In the present approach the filter width ϵ is treated as a parameter. The value of this parameter is to be prescribed in advance, and one obtains a numerical solution depending on ϵ. Figs. 1–3 show that mean results depend weakly upon ϵ if ϵ is taken larger than a threshold value (depending on the grid size and the Reynolds number). In this paper, ϵ has been determined by trail and error. In future, we want to determine ϵ from the requirement that the vortex stretching has to stop at the scale set by the grid. According to the Navier–Stokes equations, the rate of change of the length of the vorticity vector integrated along a material curve Γ is given by $\int_\Gamma \omega \cdot (\mathscr{C}(\omega,u) - \mathscr{D}(\omega))\,\mathrm{d}\Gamma$. This integral should be non-positive for the component varying at the grid scale to keep the flow on the grid. If the grid is too coarse for this to hold, that is if sub-grid scales are produced by vortex-stretching, we modify the convective operator and require that

$$\omega_\kappa \cdot (\mathscr{C}_n(\omega,u) - \mathscr{D}(\omega))_\kappa \leqslant 0, \tag{31}$$

where κ denotes the component that varies at the grid scale; for a uniform grid with spacing h this component is given by the highest representable Fourier-mode, e.g. $\omega_\kappa = \hat{\omega}_\kappa e^{\mathrm{i}\kappa x}$ with $\kappa = \pi/h$. Note: an explicit expression for $\mathscr{C}_n(\omega,u)_\kappa$ can be deduced from Eq. (22). Given a filter, the left-hand side of (31) can be evaluated for any value of the filter width ϵ (at the time-level at which the numerical solution has just been computed). For convenience, we restrict ourselves to a uniform grid here. If the Rayleigh quotient of the stretching at the grid-scale is denoted by $\lambda_\kappa(\epsilon) = \omega_\kappa \cdot \mathscr{C}_n(\omega,u)_\kappa / \omega_\kappa \cdot \omega_\kappa$, the admissible values of ϵ follow dynamically from the requirement that

$$\lambda_\kappa(\epsilon) - \frac{\kappa^2}{Re} \leqslant 0, \tag{32}$$

where the threshold value is obtained by taking the equality-sign in (32). It may be noted that this threshold is determined unambiguously if $\lambda_\kappa(\epsilon)$ decreases monotonic with respect to ϵ. If we further assume that the ratio of vortex stretching to vortex dissipation decreases with the wave-number κ, we obtain that the threshold value decreases if the grid size decreases (at $Re = \text{constant}$). This is line with our observations: at $Re_\tau = 180$ for example, the value of the effective filter width ϵ of the very coarse grid simulation ($16 \times 16 \times 8$) is four times the value of the finer grid simulation ($32 \times 32 \times 16$).

References

[1] Spalart PR. Strategies for turbulence modelling and simulations. Int J Heat Fluid Flow 2000;21:252–63.

[2] Zhou Y, Hossain M, Vahala G. A critical look at the use of filters in large eddy simulation. Phys Lett A 1989;139:330–2.

[3] Guermond JL, Oden JT, Prudhomme S. Mathematical perspectives on large eddy simulation models for turbulent flows. J Math Fluid Mech 2004;6:194–248.

[4] Carati D, Winckelmans GS, Jeanmart H. Exact expansions for filtered-scales modelling with a wide class of LES filters. In: Voke P et al., editors. Direct and large-Eddy simulation III. Dordrecht: Kluwer Academic Publisher; 1999. p. 213–24.

[5] Vreman B. Direct and large-eddy simulation of the compressible turbulent mixing layer. PhD thesis, University of Twente: The Netherlands; 1995.

[6] Leonard A. Large-eddy simulation of chaotic convection and beyond. AIAA Paper 97-0204; 1997.

[7] Ghosal S. Mathematical and physical constraints on large-eddy simulation of turbulence. AIAA J 1999;37:425–33.

[8] Sagaut P. Large Eddy simulation for incompressible flows. Berlin: Springer; 2001.

[9] Leray J. Sur le movement d'un liquide visqueux emplissant l'espace. Acta Math 1934;63:193–248.

[10] Cheskidov A, Holm DD, Olson E, Titi ES. On a Leray-α model of turbulence. Proc Roy Soc London Ser A: Math, Phys Eng Sci 2005;461:629–49.

[11] Holm DD, Marsden JE, Ratiu TS. The Euler–Poincaré equations and semidirect products with applications to continuum theories. Adv Math 1998;137:1–81.

[12] Montgomery DC, Pouquet A. An alternative interpretation for the Holm alpha model. Phys Fluids 2002;14:3365–6.

[13] Marsden JE, Shkoller S. The anisotropic Lagrangian averaged Euler and Navier–Stokes equations. Arch Rat Mech Anal 2003;166:27–46.

[14] Foias C, Holm DD, Titi ES. The Navier–Stokes-alpha model of fluid turbulence. Physica D 2001;152:505–19.

[15] Geurts BJ, Holm DD. Regularization modeling for large-eddy simulation. Phys Fluids 2003;15:L13–6.

[16] Verstappen RWCP, Veldman AEP. Symmetry-preserving discretization of turbulent flow. J Comp Phys 2003;187:343–68.

[17] Foias C, Manley O, Rosa R, Temam R. Navier–Stokes equations and turbulence. Cambridge: University Press; 2001.

[18] Vukadinovic J. Density of global trajectories for filtered Navier–Stokes equations. Nonlinearity 2004;17:953–74.

[19] Truesdell C. Two measures of vorticity. J Rat Mech Anal 1953;2:173–217.

[20] Chorin AJ, Marsden JE. A mathematical introduction to fluid mechanics. New York: Springer; 1979.

[21] Stolz S, Adams NA. An approximate deconvolution procedure for large-eddy simulation. Phys Fluids 1999;11:1699–701.

[22] Winckelmans GS, Wray AA, Vasilyev OV, Jeanmart H. Explicit-filtering large-eddy simulation using the tensor-diffusivity model supplemented by a dynamic Smagorinsky term. Phys Fluids 2001;13:1385–403.
[23] Clark RA, Ferziger JH, Reynolds WC. Evaluation of subgrid-scale models using an accurately simulated turbulent flow. J Fluid Mech 1997;91:1–16.
[24] Kim J, Moin P, Moser R. Turbulence statistics in fully developed channel flow at low Reynolds number. J Fluid Mech 1987;177:133–66.
[25] Moser RD, Kim J, Mansour NN. Direct numerical simulation of turbulent channel flow up to Re_τ=590. Phys Fluids 1999;11:943–5.
[26] Pope SB. Turbulent flows. Cambridge: University Press; 2000.